Available online at www.sciencedirect.com
ScienceDirect
Trans. Nonferrous Met. Soc. China 25(2015) 3461−3466
Transactions of Nonferrous Metals Society of China
www.tnmsc.cn

Leaching kinetics of gold bearing pyrite in H_2SO_4−$Fe_2(SO_4)_3$ system

Shui-ping ZHONG[1,2,3]

1. Zijin Mining Group Co. Ltd., Shanghang 364200, China;
2. College of Zijin Mining, Fuzhou University, Fuzhou 350108, China;
3. State Key Laboratory of Comprehensive Utilization of Low-Grade Refractory Gold Ores, Shanghang 364200, China

Received 11 January 2015; accepted 18 June 2015

Abstract: Gold bearing pyrite leaching was conducted in H_2SO_4−$Fe_2(SO_4)_3$ system at different reaction temperatures, with different ferric ion concentrations, sulfuric acid concentrations and stirring speeds. The leaching kinetics and mechanism were studied. When the temperature ranged between 30−75 °C, the pyrite leaching was mainly controlled by chemical reaction with positive correlation to the ferric ion concentration. The activation energy obtained from Arrhenius empirical formula is 51.39 kJ/mol. The EDS and XPS analyses suggest that the oxidation of sulfur within pyrite is through a series of intermediate stages, and eventually is oxidized to sulphate accompanied with the formation of element sulfur. This indicates a thiosulfate oxidation pathway of the gold bearing pyrite oxidation in H_2SO_4−$Fe_2(SO_4)_3$ system.

Key words: gold bearing pyrite; H_2SO_4−$Fe_2(SO_4)_3$ system; leaching kinetics; activation energy; sulfur oxidation

1 Introduction

Pyrite (FeS_2) is the most abundant sulfide mineral, mostly found in magmatic and igneous rocks, sedimentary and hydrothermal deposits [1]. Its frequently undesirable is associated with economical sulfide minerals, such as chalcopyrite, sphalerite and noble metals like gold, necessitating costly separation processes like roasting, flotation and bio-leaching [2,3].

Bio-leaching processes have attracted attention in the mineral processing due to their environmental acceptability, low operating costs and flexibility in adaptation [4]. Bacterial leaching of pyrite consists of two sub-processes. Firstly, pyrite is chemically oxidized to sulphate with ferric iron reduced to ferrous. Then, ferric iron is regenerated by the bacterial oxidation of ferrous iron with oxygen [5]. Several decades of exhaustive researches have been conducted to identify the kinetics of pyrite oxidation using techniques available in sterile chemical oxidation in ferric sulphate or other solutions, including solution chemistry [6], electrochemistry [1,7], spectroscopic techniques [8]. Consistent results were found with increasing the ferric concentration, resulting in an increased rate of pyrite oxidation, while increasing the ferrous iron and hydrogen ion concentrations inhibited the rate of chemical oxidation. For Carlin-type gold ores, low gold cyanidation rate was obtained since it contained gold-bearing pyrite. The main objective of this work is to obtain the rate determining factors, in particular the leaching operation parameters (temperature, ferric iron concentration and acidity), for gold-bearing pyrite to achieve greater dissolution rate and reduced oxidation time.

2 Experimental

2.1 Sample preparation and characterization

Gold-bearing pyrite from Shuiyindong Gold Ore in Guizhou province, China, was selected for the gold concentrate. After sieving to fractions 150−250 μm, pyrite was firstly immersed in HCl for 3 h to remove all oxidation products and flotation agents from the mineral surface, and then washed with acetone three times. It was subsequently rinsed with distilled water and vacuum dried at 50 °C for approximately 2 h. The final sample was stored before analysis. Sample characterization was carried out by X-ray diffraction (XRD) with Cu K_α radiation over a 2θ range of 10°−90° at a scan speed of

Foundation item: Project (51474075) supported by the National Natural Science Foundation of China
Corresponding author: Shui-ping ZHONG; Tel: +86-597-3315966; E-mail: zhongshuiping01@163.com
DOI: 10.1016/S1003-6326(15)63983-8

0.004 (°)/s. The main phase is pyrite and no quartz is detected after the treatment (Fig. 1). This was confirmed by scanning electron microscopy (SEM) observation shown in Fig. 2, which shows pyrite with very fine size distribution and free of other ultrafine particles adhering to the particle surface. The chemical analysis gave an element composition of 43.68% Fe, 51.60% S, 3.06% As and 0.005479% Au (mass fraction). The surface analysis by X-ray photoelectron spectroscopy (XPS) (a VG 36 Escalab MKII spectrometer with Al K_α radiation with a source power of 15 kV and 10 mA and chamber pressure lower than 5×10^{-9} Pa) shows no oxidation products.

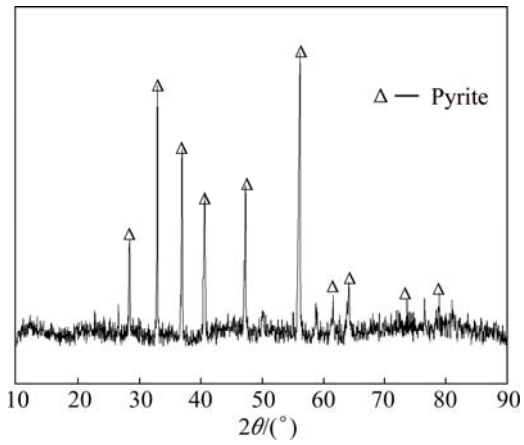

Fig. 1 XRD pattern of gold-bearing pyrite

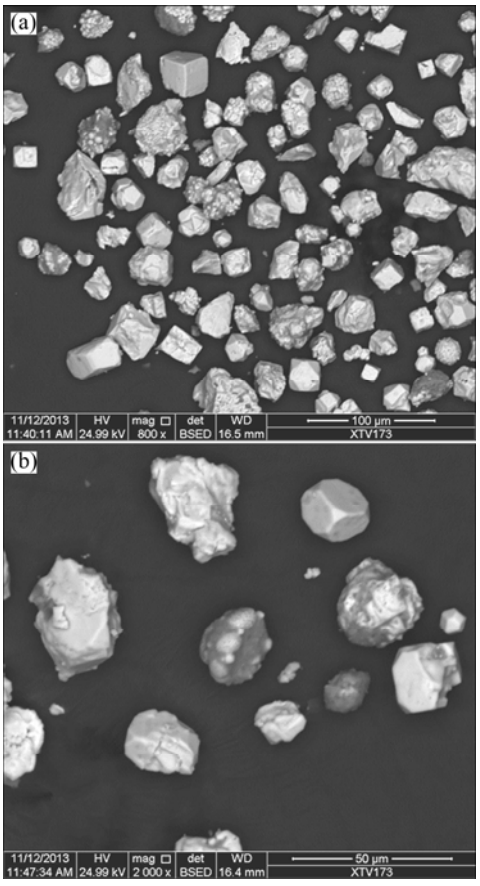

Fig. 2 SEM images of gold-bearing pyrite

The pyrite is of high purity with uniform particle size distribution and smooth surface. The failure to remove these fines, sharp edges, damaged zones and air-caused oxidation products formed on the grain surfaces during grinding can lead to anomalous initial dissolution rates during experiment [9]. All solutions were prepared by dissolving $Fe_2(SO_4)_3$ as the oxidant into distilled water. The concentration of ferric was determined by potassium dichromate titration. The initial pH value and the redox potential of solution were adjusted to the corresponding values by the additions of H_2SO_4 and $FeSO_4\cdot7H_2O$.

2.2 Experimental setup and procedure

The experiment was carried out in a 1000 mL round bottom flask with continuous stirring, equipped with sampling port, and pH value and redox potential measuring devices. The temperature was maintained (±0.5 °C) in thermostat water bath. As soon as the reactor reached the required temperature, a known quantity of pyrite was added. When leaching was completed, solid residue was obtained after filtration and washed with distilled water. The sample was then dried for subsequent characterization. Variable reaction progress for pyrite dissolution was determined through the inspection of the sulfide ion in the solid residue. This kind of test method is more accurate than measuring iron and sulfur concentrations in solution due to precipitation during the experiment. Four different parameters: temperature, stirring rate, ferric iron concentration and acidity were studied for the dissolution kinetics of pyrite. The initial redox potential and mineral concentration were set as 725 mV (vs SHE) and 10 g/L. The redox potential was continuously monitored with an oxidation−reduction potential (ORP) potentiometer (Ag/AgCl electrodes filled with 3.5 mol/L saturated KCl solution, 205 mV vs SHE, supplied by HACH in USA).

3 Results and discussion

3.1 Influence of temperature on pyrite dissolution

The apparent activation energy for pyrite dissolution is obtained from the Arrhenius law:

$$k=A\mathrm{e}^{-E_a/RT} \quad (1)$$

where k is the rate constant, A is the pre-exponential factor, E_a is the apparent activation energy, R is the gas constant and T is the absolute temperature (K). To obtain the apparent activation energy, the experiments were carried out at four different temperatures of 30, 45, 60 and 75 °C with the ferric concentration of 30 g/L. The leaching rate of pyrite significantly increases with increasing the temperature (Fig. 3). The apparent activation energy for pyrite oxidation by ferric obtained

from the pyrite dissolution is 51.39 kJ/mol (Fig. 4). The increased stirring speed above 200 r/min shows no significant effect on the rate of leaching (Fig. 5). Similar result was also found by LONG and DIXON [10] with stirring speeds of 650, 800 and 950 r/min. There was no remarkable effect of stirring speed above 800 r/min on the rate of dissolution.

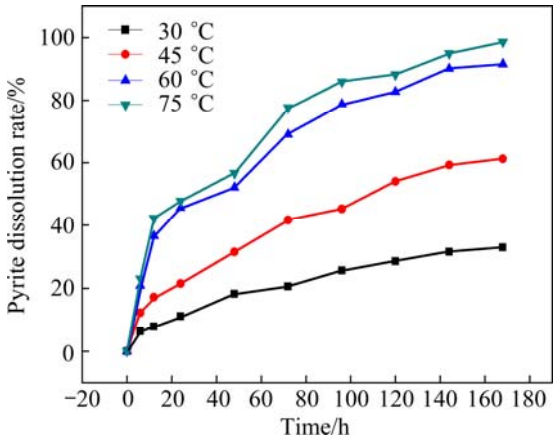

Fig. 3 Pyrite dissolution at different temperatures (φ=725 mV, pH=1.0, 400 r/min)

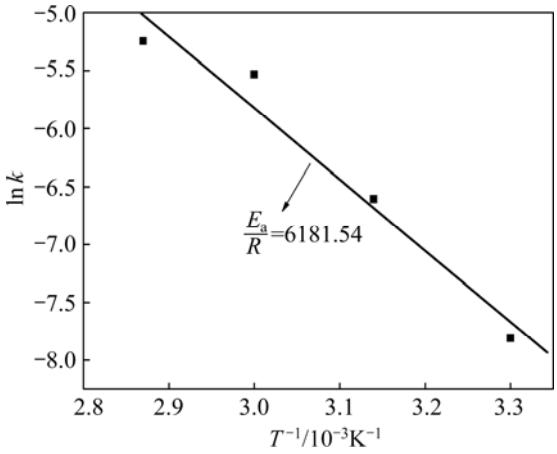

Fig. 4 ln k versus ($1/T$) for pyrite dissolution (φ=725 mV, pH=1.0, 400 r/min)

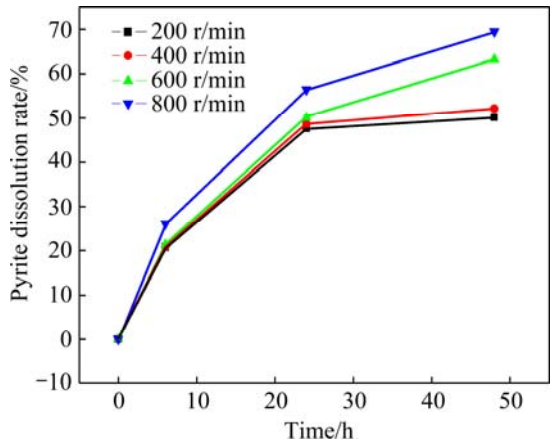

Fig. 5 Pyrite dissolution under different stirring speeds (t=75°C, φ=725 mV, pH=1.0)

Researches have been done on pyrite dissolution with ferric iron as the oxidant in a series of acidities, grain diameters and temperatures. The range of activation energy (33−92 kJ/mol) was reported, which suggested the oxidation process was controlled by chemical or electrochemical reaction but not by physical or diffusion reaction. It was a chemical reaction process in which molecular adsorption reactions happened on the pyrite surface or a electrochemical reaction process with electron transfering from the cathodic sites to the distinct anodic sites on the pyrite surface. WIERSMA and RIMSTIDT [11] examined on $FeCl_3$ solution and derived an activation energy of 92 kJ/mol in an acidic environment. NICHOLSON et al [12] reported an activation energy of 88 kJ/mol in a neutral environment. HOLMES and CRUNDWELL [1] used the electrochemical technique of potentiometry to study the kinetics of the reaction through measuring the mixed potential of a sample of corroding pyrite in solution with different compositions. It has been proved that both the observation of half-order kinetics and the oxygen in sulphate product arising from water were a direct consequence of the electrochemical mechanism.

There are essential different mechanisms between electrochemical and chemical reactions. For the electrochemical reaction, the reactants do not directly contact but collide with an electronically conducting substrate. While for the chemical reaction, the reactants collide directly to form the product. At the same time, LI et al [13] considered that it was hard to separate electrochemical reactions from heterogeneous chemical reactions occurring at a solid−liquid interphase.

The magnitude of the activation energy means that temperature is the key factor for pyrite dissolution. Combined with the fact that there is no apparent effect of stirring on the oxidation rate (Fig. 5), the process of pyrite oxidation is suggested to be controlled by chemical reaction but not by diffusion reaction.

3.2 Influence of oxidant concentration on pyrite dissolution

Figure 6 shows the variation of leaching rate in different initial ferric iron concentrations of 8−40 g/L. It is apparent that the leaching rate of pyrite increases with increasing the oxidant concentration.

The reaction order can be evaluated using the following expression:

$$v_A=-dc_A/dt=k_Ac_A^n \quad (2)$$

Equation (2) can be transformed to logarithmic form:

$$\lg v_A=\lg k_A+n\lg c_A \quad (3)$$

where v_A is the reaction rate at different concentrations

(c_A), k_A is the rate constant of pyrite dissolution and n is the reaction order. Figure 7 shows that the reaction order is constant at a value of 0.36 with the initial ferric ion concentrations ranging from 8 to 40 g/L.

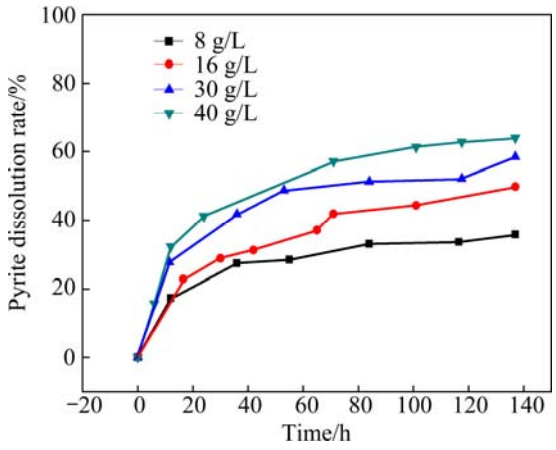

Fig. 6 Pyrite dissolution under different ferric ion concentrations (t=75 °C, φ=725 mV, pH=1.0, 400 r/min)

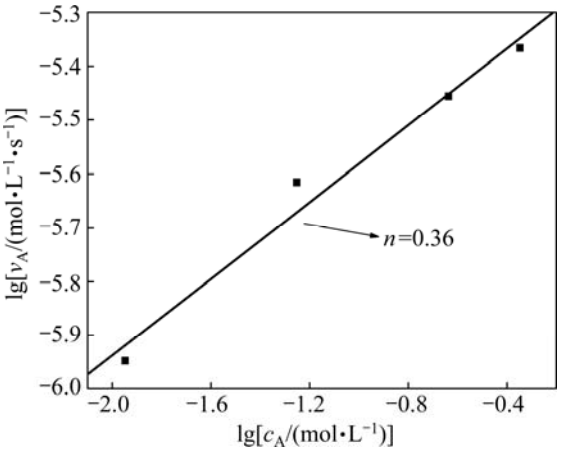

Fig. 7 Reaction order under different ferric ion concentrations (t=75 °C, φ=725 mV, pH=1.0, 400 r/min)

The leaching rates are generally influenced by the particle size, redox potential, type of oxidant, concentration and surface area, pressure and temperature [14]. All of these, redox potential is the most critical factor for the leaching process. The redox potential in solution plays a very important role in controlling the pyrite dissolution rate by ferric iron. The redox potential depends on both Fe^{3+} and Fe^{2+} concentrations, the value is given by Nernst equation [15].

Former research also held different views on the controlling processes of pyrite leaching rate. Using samples from several places to study pyrite dissolution, CHANDRA and GERSON [15] suggested that the instantaneous rate was determined by the adsorption of ferric and ferrous on the pyrite surface, while SINGER and STUMM [16] proved that the reaction rate was controlled by ferrous oxidation to generate ferric in a cyclic leaching process.

Figure 8 shows the influence of the acidity (the concentration of H_2SO_4) on the pyrite oxidation. It can be seen that the acidity (6−47 g/L) has no significant effect on the pyrite leaching rate with the initial ferric ion concentration of 8 g/L. In addition, GARRELS et al [17] confirmed that the pH value did not play a significant influence on the dissolution rate with the pH value range of 0−2. However, it may be remarkable at higher pH value.

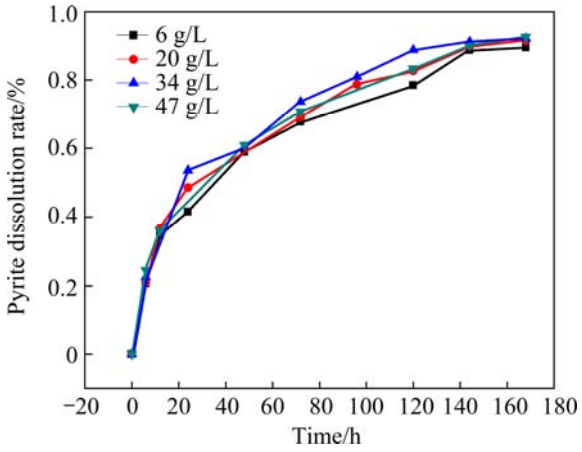

Fig. 8 Pyrite dissolution under different concentrations of H_2SO_4) (t=75 °C, φ=725 mV, pH=1.0, 400 r/min)

3.3 Proposal reaction mechanism

Despite all the previous efforts, no conclusion has yet emerged on a well-established oxidation mechanism. According to SINGER and STUMM [16], pyrite oxidation by ferric can be described as

$$FeS_2+14Fe^{3+}+8H_2O\longrightarrow 15Fe^{2+}+2SO_4^{2-}+16H^+ \quad (4)$$

SASAKI [18] examined a sulfur-rich layer on a pyrite surface oxidized in ferric medium. LUTHER [19] proposed that the sulfur layer was not a direct oxidation product, but came from the decomposition of thiosulfate into element sulfur and bisulfite according to the following formula:

$$8S_2O_3^{2-}+8H^+\longrightarrow S_8+8HSO_3^- \quad (5)$$

Few studies have focused on the aqueous sulfur chemistry, probably because of analytical difficulties or detection error. The pyrite leaching in solution resulted in the production of ferrous iron and sulfate. Other species, for instance, hydrogen sulfide, sulfur, polysulfides, ferric hydroxide, oxyhydroxide and ferric oxide may also form. Intermediate products such as sulfite, thiosulfate and polythionates were also generated during the experiment.

In this study, the leaching experiment was conducted in acidic media to avoid any iron hydrolysis and precipitation. Under this controlled condition, the

reaction mechanism was studied. The XRD patterns of pyrite before and after leaching at different dissolution rates are shown in Fig. 9. With increasing the pyrite dissolution, the characteristic peak of element sulfur becomes stronger. At the highest pyrite dissolution (82%), the peaks of pyrite are weak and elemental sulfur is the main phase. Energy dispersion spectroscopy (EDS) analysis was carried out on the particle of pyrite. Table 1 shows that the sulphur content on the pyrite after leaching is higher than that on the pyrite before leaching. This sulphur can be associated with either the presence of a thin layer of element sulphur on the pyrite or the formation of intermediate. In the XPS spectra (Fig. 10), S^0 precipitates and SO_4^{2-} are detected on the pyrite surface, but other valence states of sulfur are not detected. According to FOWLER and CRUNDWELL [20], Fe^{3+} splits the chemical bonds of iron and sulfur in pyrite lattice and injects holes into t2g orbit during the oxidation process. Those holes can split H_2O and form OH^- which has strong oxidation characteristics and react with sulfur valence band, thus the S^{2-} of pyrite is oxidized. Sulfur is eventually oxidized into sulfate radical through a series of intermediate forms with the generation of some element sulfur. Therefore, a simplest expected oxidation mechanism is proposed and the formation of $S_2O_3^{2-}$ is the key intermediate conversion step for the oxidation process.

Table 1 EDS results of pyrite (mass fraction, %)

Before leaching		After leaching		
Fe	S	Fe	S	O
46.38	51.00	7.81	54.12	34.40

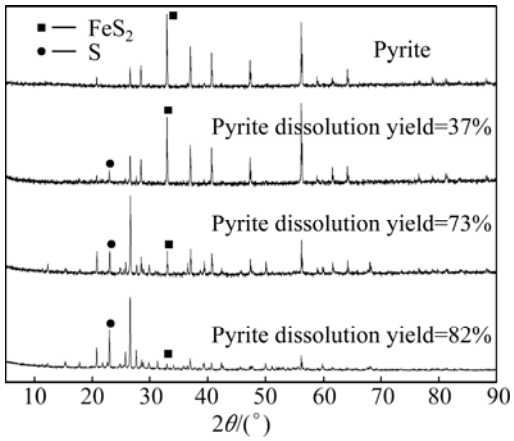

Fig. 9 XRD pattern of pyrite at different dissolution rates

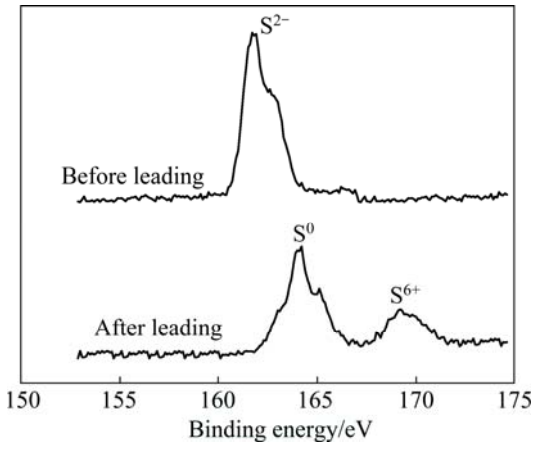

Fig. 10 XPS spectra of pyrite before and after leaching

4 Conclusions

In H_2SO_4−$Fe_2(SO_4)_3$ system, at the temperature range of 30−75 °C, pyrite leaching is mainly controlled by chemical reaction with positive correlation to the ferric ion concentration. The activation energy obtained from Arrhenius empirical formula is 51.39 kJ/mol. The EDS and XPS analyses show that the oxidation of sulfur is through a series of intermediate stages, and eventually oxidized to sulphate and accompanied with the formation of some element sulfur. This is indicated that the mechanism of pyrite leaching pathway is via thiosulfate oxidation.

References

[1] HOLMES P R, CRUNDWELL F K. The kinetics of the oxidation of pyrite by ferric ions and dissolved oxygen: An electrochemicalstudy [J]. Geochimica Cosmochimica Acta, 2000, 64(2): 263−274.

[2] XIAO Chun-qiao, CHI Ru-an, FANG Yu-juan. Effects of *Acidiphilium cryptum* on biosolubilization of rock phosphate in the presence of *Acidithiobacillus ferrooxidans* [J]. Transactions of Nonferrous Metals Society of China, 2013, 23(7): 2153−2159.

[3] XIA Jin-lan, ZHAO Xiao-juan, LIANG Chang-li, NIE Zhen-yuan, TANG Lu, MA Chen-yan, ZHENG Lei, ZHAO Yi-dong, QIU Guan-zhou. Sulfur speciation transformation during bioleaching of pyrite-containing sphalerite concentrate by thermophile sulfolobus metallicus at 65 °C [J]. Journal of Central South University of Technology, 2012, 19(7): 1961−1966.

[4] GU Guo-hua, SU Li-jun, CHEN Ming-lian, SUN Xiao-jun, ZHOU Hong-bo. Bio-leaching effects of Leptospirillum ferriphilum on the surface chemical properties of pyrite [J]. Mining Science and Technology, 2010, 20(2): 286−291.

[5] BOON M, HEIJNEN J J. Chemical oxidation kinetics of pyrite in bioleaching processes [J]. Hydrometallurgy, 1998, 48(1): 27−41.

[6] ZHAO Zhong-wei, LI Hong-gui, SUN Pei-mei, LI Yun-jiao, HUO Guang-sheng. Effect of processing history of pyrite on its leaching kinetics [J]. Transactions of Nonferrous Metals Society of China, 2003, 13(2): 443−447.

[7] LIU Run-qing, SUN Wei, HU Yue-hua, WANG Dian-zuo. Effect of organic depressant lignosulfonate calcium on separation of chalcopyrite from pyrite [J]. Journal of Central South University of Technology, 2009, 16(5): 753−757.

[8] McGUIRRE M M, JALLAD K N, AMOTZ D B, HAMERS R J. Chemical mapping of elemental sulfur on pyrite and arsenopyrite surfaces using near-infrared Raman imaging microscopy [J]. Applied Surface Science, 2001, 178(1−4): 105−115.

[9] McKIBBEN M A, TALLANT B A, del ANGEL J K. Kinetics of inorganic arsenopyrite oxidation in acidic aqueous solutions [J]. Applied Geochemistry, 2008, 32(2): 121−135.

[10] LONG H, DIXON D G. Pressure oxidation of pyrite in sulfuric acid media: A kinetic study [J]. Hydrometallurgy, 2004, 73(3−4): 335−349.
[11] WIERSMA C L, RIMSTIDT J D. Rates of reaction of pyrite and marcasite with ferric iron at pH 2 [J]. Geochimica et Cosmochimica Acta, 1984, 48(1): 85−92.
[12] NICHOLSON R V, GILLHAM R W, REARDON E J. Pyrite oxidation in carbonate-buffered solution: 2. Rate control by oxide coatings [J]. Geochimica et Cosmochimica Acta, 1990, 54(2): 395−402.
[13] LI Wei-zhong, QIN Wen-qing, SUN Wei, QIU Guan-zhou. Electrodeposition of dixanthogen (TETD) on pyrite surface [J]. Transactions of Nonferrous Metals Society of China, 2007, 17: 154−158.
[14] LIU San-jun, QIN Wen-qing, SUN Wei, ZHONG Shui-ping, CHEN Bo. Electrode redox reaction kinetics of xanthate on pyrite surface [J]. The Chinese Journal of Nonferrous Metals, 2013, 23(4): 1114−1118. (in Chinese)
[15] CHANDRA A P, GERSON A R. The mechanisms of pyrite oxidation and leaching: A fundamental perspective [J]. Surface Science Reports, 2010, 65(9): 293−315.
[16] SINGER P C, STUMM W. Acid mine drainage: The determing step [J]. Science, 1970, 167: 1121−1123.
[17] GARRELS R M, THIMPSON M E. A chemical model for sea water as 25 °C and one atmosphere total pressure [J]. American Journal of Science, 1962, 260: 57−66.
[18] SASAKI K. Effect of grinding on the rate of oxidation of pyrite by oxygen in acid solutions [J]. Geochimca et Cosmochimica Acta, 1994, 58(21): 4649−4655.
[19] LUTHER G W. Pyrite oxidation and reduction: Molecular orbital theory considerations [J]. Geochimica et Cosmochimica Acta, 1987, 51(12): 3193−3199.
[20] FOWLER T A, CRUNDWELL F K. Leaciting of zinc sulfide by thiobacillus ferrooxidans: Experiments with a controlled redox potential indicate no direct bacterialmechanism [J]. Applied Environmental Microbiology, 1998, 64: 3570.

在 H_2SO_4−$Fe_2(SO_4)_3$ 体系中载金黄铁矿浸出动力学

袁水平 [1,2,3]

1. 紫金矿 业集团股份有限公司，上杭 364200；
2. 福州大学 紫金矿业学院，福州 350108；
3. 低品位难处理黄金资源综合利用国家重点实验室，上杭 364200

摘 要：在 H_2SO_4−$Fe_2(SO_4)_3$ 体系中研究载金黄铁矿的浸出动力学，探讨反应温度、Fe^{3+}浓度、硫酸浓度、搅拌速度等对黄铁矿浸出的影响规律。结果表明：在 H_2SO_4−$Fe_2(SO_4)_3$ 体系中，在 30~75 °C 下黄铁矿浸出过程主要受化学反应控制 Fe^{3+}浓度与黄铁矿的浸出呈正相关，通过 Arrhenius 经验公式求得浸出表观活化能为 51.39 kJ/mol。EDS 与 XPS 分析结果表明：黄铁矿氧化过程中硫的氧化经一系列中间形态，最终被氧化成硫酸根，并伴有部分元素硫生成，符合硫代硫酸根氧化路径机理。

关键词：载金黄铁矿；H_2SO_4−$Fe_2(SO_4)_3$ 体系；浸出动力学；活化能；硫氧化

(Edited by Mu-lan QIN)